Biosensors and Bioelectronics 42 (2013) 467–473

Contents lists available at SciVerse ScienceDirect

Biosensors and Bioelectronics

journal homepage: www.elsevier.com/locate/bios

# An ultra-high sensitive platform for fluorescence detection of micrococcal nuclease based on graphene oxide

Yue He, Ling-Hong Xiong, Xiao-Jing Xing, Hong-Wu Tang*, Dai-Wen Pang

*Key Laboratory of Analytical Chemistry for Biology and Medicine (Ministry of Education), College of Chemistry and Molecular Sciences, Research Center for Nanobiology and Nanomedicine (MOE 985 Innovative Platform), Wuhan Institute of Biotechnology, and State Key Laboratory of Virology, Wuhan University, Wuhan 430072, China*

ARTICLE INFO

*Article history:*
Received 30 June 2012
Received in revised form
30 September 2012
Accepted 11 October 2012
Available online 23 October 2012

*Keywords:*
Graphene oxide
Fluorescence
MNase
Single-stranded DNA

ABSTRACT

Micrococcal nuclease (MNase) is the extracellular nuclease of *Staphylococcus aureus* (*S. aureus*). It preferentially digests single-stranded nucleic acids. The existence of MNase can be the standard to identify *S. aureus* and the content of MNase can be used to evaluate the pathogenicity of *S. aureus*. Herein, an ultra-high sensitive and selective fluorescent sensing platform for MNase is developed based on MNase-induced DNA strand scission and the difference in affinity of graphene oxide (GO) for single-stranded DNA containing different numbers of bases in length. In the absence of MNase, the adsorption of the dye-labeled ssDNA on GO makes the dyes close proximity to GO surface resulting in high efficiency quenching of fluorescence of the dyes. Conversely, and very importantly, in the presence of MNase, it cleaves the dye-labeled ssDNA into small fragments. The introduction of GO into the sensing solution results in weak quenching of the fluorescence of the dyes due to the weak affinity of the short dye-labeled oligonuleotide fragment to GO, and the fluorescence intensity gradually increases with increasing concentration of MNase. MNase can be detected in a range of $8\times10^{-5}$ to $1.6\times10^{-3}$ unit/mL with a detection limit of $2.7\times10^{-5}$ unit/mL and good selectivity. The detection limit is of two orders of magnitude lower than those reported fluorescence MNase assays. Moreover, when the GO-based biosensor is used in *S. aureus* sample assays, preeminent fluorescence signals are obtained, thus the platform of the GO-based biosensor can be used to detect MNase in real-world samples.



## 1. Introduction

Nucleases are a family of enzymes that can cleave the phosphodiester bonds between the nucleotide subunits of nucleic acids. The cleavage reactions of DNA(RNA) that catalyzed by nucleases play key roles in a variety of fields ranging from biotechnology to pharmacology, as well as in biological processes involving replication, recombination, DNA repair, molecular cloning, genotyping, and mapping (Arber, 1978; Pingoud and Jeltsch, 2001; Wright et al., 2005; Nishino and Morikawa, 2002; Stoerker et al., 2000; Norberg et al., 2006; Zeevi et al., 2008; Allan et al., 2012). Hence the assay of nucleases is of high importance for the development of efficient therapeutics and drug discovery. Traditional techniques, including gel electrophoresis (Rosenthal and Lacks, 1977), high-performance liquid chromatography (HPLC) (Bouriotis et al., 1987), enzyme-linked immunosorbent assay (ELISA) (Hiramatsu et al., 1998), and radioactive labeling (Smith and Anslyn, 1994) have been established to monitor nuclease activity. However, these assay methods share the drawbacks of being complicated, time-consuming, laborious, and require sophisticated instrumentation or isotope labeling. Recently, colorimetric methods based on conjugated polymers (Tang et al., 2006) and gold nanoparticles (Song et al., 2009; Cao et al., 2011; Liu et al., 2012; Xu et al., 2007) have been developed to study DNA cleavage. Although promising, these techniques suffer from intrinsic limitations such as the sophisticated synthesis processes, the need of functionalizing thiol (or dye)-modified oligonucleotide probes or the critical operation conditions. To address these limitations, fluorescence assays based on fluorescence resonance energy transfer (FRET) technology have been applied and developed because of their intrinsic high sensitivity and selectivity, among which quantum dots (QDs) (Huang et al., 2008; Qiu et al., 2010) and conjugated polymers (Pu et al., 2010; Zhang et al., 2009; Feng et al., 2009) have often been used in nuclease detection assays. However, these strategies are compromised to expensive double fluorophore-labeled DNA substrates, complicated synthesis procedure, polydispersity of conjugated polymers and usually having a high background signal because of the low energy transfer efficiency between the donor and the acceptor. Therefore, to overcome these shortcomings, the development of a simple and sensitive method for nuclease analysis should be of general interest.

As a kind of promising single-atomthick and two-dimensional nanomaterial, graphene has received much attention for its

* Corresponding author. Tel.: +86 27 68756759; fax: +86 27 68754685.
*E-mail address:* hwtang@whu.edu.cn (H.-W. Tang).

0956-5663/$ - see front matter © 2012 Elsevier B.V. All rights reserved.
http://dx.doi.org/10.1016/j.bios.2012.10.045

remarkable electronic, mechanical, and thermal properties (Novoselov et al., 2004; Geim and Novoselov, 2007). Due to its peculiar electronic properties, the water-soluble derivative of graphene, graphene oxide (GO), is an excellent energy acceptor in resonance energy transfer which makes the fluorescent detection a promising application of GO in sensing technology (Swathi and Sebastian, 2008, 2009). In addition, GO can nonconvalently interact with single-stranded DNA (ssDNA) by π–π stacking interactions between nucleotide bases and GO, but hardly interacts with rigid double-stranded DNA (dsDNA) or aptamer–target complexes (Lu. et al., 2009, 2010a, 2010b; Chang et al., 2010). Therefore, GO as an excellent energy acceptor has been reported for detecting nucleases (Lu et al., 2011; Lee and Min, 2012). Lu and coworkers first designed Y-shaped DNA (Y-DNA) as the multiplex probe for the multiplex detection of nucleases by using GO as a platform (Lu et al., 2011). Subsequently, Lee and coworkers developed an exonuclease detection method based on the preferential binding of single-stranded DNA (ssDNA) over double-stranded DNA (dsDNA) to GO (Lee and Min, 2012). These fluorescence assays based on GO have shown great advantages. However, two of these cleavage assays were designed only for nucleases whose substrates are dsDNA molecules. The development of a GO-based biosensor for nucleases whose substrates are ssDNA molecules are also required. Very recently, Zhao (Zhao et al., 2011) made a detailed investigation on the difference in affinity of GO for ssDNA containing different numbers of bases in length and proved that short ssDNA had weaker affinity to GO than long ssDNA.

Herein, a simple, rapid and ultra-high sensitive GO-based sensing platform is constructed for fluorescence detection of nuclease whose substrates is ssDNA activity. By taking the advantage of the difference in affinity of GO for ssDNA containing different numbers of bases in length, micrococcal nuclease (MNase), an extracellular nuclease, which could preferentially digest single-stranded DNA at AT-rich regions at slightly basic pH (Fox and Waring, 1987), is taken as the model enzyme to provide the "proof-of-principle" verification of this method. The FAM-labeled 20-mer ssDNA (5′-FAM-TATATGGATGATGTGGTATT-3′) is used as the nuclease substrate. In the absence of MNase, the adsorption of the FAM-labeled 20-mer ssDNA on GO makes the dyes close proximity to GO surface resulting in high efficiency quenching of fluorescence of the dyes. Conversely, in the presence of MNase, the FAM-labeled 20-mer ssDNA is hydrolyzed into small fragments, the introduction of GO into the sensing solution results in weak quenching of the fluorescence of the FAM due to the weak affinity of the short FAM-linked oligonuleotide fragment to GO, and the fluorescence intensity gradually increases with increasing concentration of MNase.

## 2. Experimental

### 2.1. Chemicals and materials

The FAM-labeled 20-mer ssDNA with a sequence of 5′-FAM-TATATGGATGATGTGGTATT-3′, FAM-labeled 10-mer ssDNA with a sequence of 5′FAM-TATATGGATG-3′, and FAM-labeled 5-mer ssDNA with a sequence of 5′FAM-TATAT-3′, were synthesized by Shanghai Sangon Biotechnology Co., Ltd. (Shanghai, China). Graphene oxide (GO) was purchased from Sinocarbon Materials Technology Co., Ltd. (China). Micrococcal nuclease (MNase) and exonuclease I were purchased from Takara Biotechnology Co., Ltd. (Dalian, China). S1 nuclease was purchased from Shanghai Sangon Biotechnology Co., Ltd. (Shanghai, China). Peptone and yeast extract were purchased from Oxoid Ltd. (England). The Tris–HCl buffer used in this experiment consisted of 20 mM Tris–HCl (pH 8.0), 5 mM NaCl and 2.5 mM $CaCl_2$. Milli-Q purified water was used to prepare all the solutions.

### 2.2. Apparatus

Fluorescent emission spectra were performed on F-4600 Fluorescence Spectrophotometer, Hitachi High-Technology Co., Ltd. (Tokyo, Japan). The sample cell was a 700-μL quartz cuvette. The luminescence intensity was monitored by exciting the sample at 480 nm and measuring the emission at 520 nm. The slits for excitation and emission were set at 5 nm, 10 nm, respectively. The fitting of the experimental data was accomplished using the software Origin 8.0.

### 2.3. Optimization of the reaction time between FAM-labeled 20-mer ssDNA and GO

The purchased GO was sonicated in Milli-Q purified water for 5 h to give a homogeneous black solution and stored at 4 °C for use. The working solution containing ssDNA was obtained by diluting the stock solution to a concentration of 40 nM using 20 mM Tris–HCl buffer. To optimize the reaction time between FAM-labeled 20-mer ssDNA and GO assays, 20 μL of the ssDNA stock solution (1 μM), and 20 μL GO solution (500 μg/mL) as prepared were mixed. The mixed solution was diluted with Tris–HCl buffer to 500 μL. The above prepared solution was incubated for 0, 1, 5, 10, 15, 20, 25, 30, 35, 40, 45, 50, 55, and 60 min at room temperature. Finally, the fluorescence intensity of the incubated solution was measured at 520 nm with excitation at 480 nm.

### 2.4. Optimization of the reaction time between FAM-labeled 20-mer ssDNA and MNase

To optimize the reaction time between FAM-labeled 20-mer ssDNA and MNase assays, 20 μL of the ssDNA stock solution (1 μM), and $4 \times 10^{-4}$ units /mL MNase solution were mixed. The above prepared solution was incubated for 0, 5, 10, 15, 20, 25, 30, 35, 40, 45, 50, 55, and 60 min at 37 °C. Then 20 μL GO solution (500 μg/mL) as-prepared was added to the solution, the mixed solution was diluted with a Tris–HCl buffer to 500 μL. The above prepared solution was incubated for 10 min at room temperature. Finally, the fluorescence intensity of the incubated solution was measured at 520 nm with excitation at 480 nm.

### 2.5. Performance of MNase detection in a Tris–HCl buffer

For MNase assays, 20 μL of the ssDNA stock solution (1 μM), and appropriate concentrations of MNase solution were mixed. The above-prepared solution was incubated for 30 min at 37 °C. Then 20 μL GO solution (500 μg/mL) as prepared was added to the solution, the mixed solution was diluted with Tris–HCl buffer to 500 μL. The above-prepared solution was incubated for 10 min at room temperature. Finally, the fluorescence intensity of the incubated solution was measured at 520 nm with excitation at 480 nm.

### 2.6. Performance of MNase detection in culture medium

For MNase in culture medium assays (250-fold diluted with a Tris–HCl buffer), 20 μL of the ssDNA stock solution (1 μM), and appropriate concentrations of MNase solution were mixed. The above-prepared solution was incubated for 30 min at 37 °C. Then 40 μL GO solution (500 μg/mL) as prepared was added to the solution, the mixed solution was diluted with culture medium solution to 500 μL. The above-prepared solution was incubated

for 10 min at room temperature. Finally, the fluorescence intensity of the incubated solution was measured at 520 nm with excitation at 480 nm.

### 2.7. *Staphylococcus aureus* sample assay

*Staphylococcus aureus* sample (*S. aureus*, CCTCC AB91093) was provided by the Chinese Center for Type Culture Collections, Wuhan University, PR China. *S. aureus* was grown in a peptone culture medium which contains 10 g/L peptone, 5 g/L yeast extract and 5 g/L NaCl (pH 7.0). The culture medium was sterilized in high-pressure steam for 30 min at 120 °C before use. Then the culture mediums containing *S. aureus* which were incubated for 0 h, 2 h, 4 h, 6 h, and 8 h were centrifuged at 5000 rpm for 5 min, respectively, and the supernatant was collected and boiled for 10 min at 95 °C. Supernatant (10-fold diluted with culture medium) (2 μL) was added into the nuclease digestion reaction buffer (458 μL) which contains 40 nM FAM-labeled 20-mer ssDNA, then 40 μL GO solution (500 μg/mL) as prepared was added to the solution after the mixed solution was incubated for 30 min at 37 °C. The above-prepared solution was incubated for 10 min at room temperature. Finally, the fluorescence intensity of the incubated solution was measured at 520 nm with excitation at 480 nm.

## 3. Results and discussion

### 3.1. Design strategy

Fig. 1 illustrates the sensing strategy for the detection of micrococcal nuclease (MNase). In the absence of target molecule (MNase), FAM-labeled 20-mer ssDNA is adsorbed onto the graphene oxide (GO) sheet by π–π stacking making the fluorophore close proximity to GO surface; thus, GO significantly quenches the fluorescence of FAM. In the presence of target molecules (MNase), the FAM-labeled 20-mer ssDNA is cut into fragments by MNase, the introduction of GO into the sensing solution results in weak quenching of the fluorescence of the FAM due to the weak affinity of the short FAM-linked oligonuleotide fragment to GO, and the fluorescence intensity gradually increases with increasing concentration of MNase. Therefore, the fluorescence intensity of FAM as a function of MNase concentration is measured correspondingly.

In order to demonstrate the feasibility of our strategy, we first investigated the fluorescence quenching efficiency of GO to ssDNA containing different numbers of bases in length. As shown in Fig. S1, the fluorescence quenching efficiency of GO to ssDNA increased with the increasing number of the bases of ssDNA. When the concentration of GO was fixed at 20 μg/mL and oligonucleotide fixed at 40 nM, we observed that the fluorescence quenching efficiency of GO to FAM-labeled ssDNA containing 20 bases (named 20-F) was 99%. In contrast, for the similar ssDNA containing five bases (named 5-F), a 46% fluorescence quenching efficiency was achieved. This phenomenon indicated that the affinity of the short ssDNA to GO is significantly weaker than that of the long ssDNA, as reported by Zhao's work (Zhao et al., 2011) which forms the basis for the design of GO-based fluorescence biosensor for MNase detection.

The process of fluorescence changing of the GO-based biosensor for MNase detection is shown by fluorescence spectra. Fig. S2 shows the fluorescence emission spectra of FAM-labeled 20-mer ssDNA under different conditions. The fluorescence spectrum of FAM-labeled 20-mer ssDNA in the Tris–HCl buffer shows strong fluorescence intensity that can be attributed to the presence of the FAM (Fig. S2, curve a). However, in the presence of GO, up to 99% quenching of the fluorescence emission was observed (Fig. S2, curve b), which indicates strong adsorption of the FAM-labeled 20-mer ssDNA on GO and high fluorescence quenching efficiency of GO. However, upon the reaction of FAM-labeled 20-mer ssDNA with $4 \times 10^{-4}$ units/mL MNase, the introduction of GO into the sensing solution exhibits significant fluorescence intensity (Fig. S2, curve c). Therefore, MNase detection could be easily realized by monitoring the change of fluorescence signal.

### 3.2. Effect of adding order

In order to achieve the best sensing performance, we first investigate the influence on the final results caused by the adding order of MNase and GO. Fig. 2A shows the result of influence on the final results caused by the adding order of MNase and GO. Fig. 2A, curve a shows that considerably high fluorescence signal of the system appears when we first mixed the FAM-labeled 20-mer ssDNA with $4 \times 10^{-4}$ units/mL MNase, the mixed solution was incubated for 30 min at 37 °C. Then 20 μg/mL GO was added and the solution was incubated for 10 min at room temperature. In contrast, in Fig. 2A, curve b, which shows the result of the reversed adding order of MNase and GO of Fig. 2A, curve a, only exhibits very low fluorescence signal. Therefore the adding order of MNase and GO has a significant influence on the final results. This phenomenon can be explained by the properties of GO which can protect DNA against enzymatic cleavage and intracellular stability of DNA compared with free DNA probes (Lu et al., 2010a,

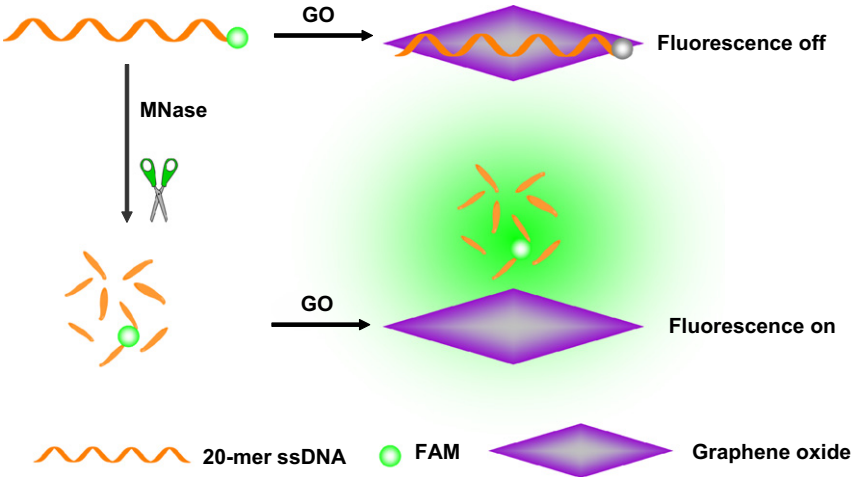


**Fig. 1.** Scheme for the mechanism of GO-based biosensor for the micrococcal nuclease (MNase) detection.

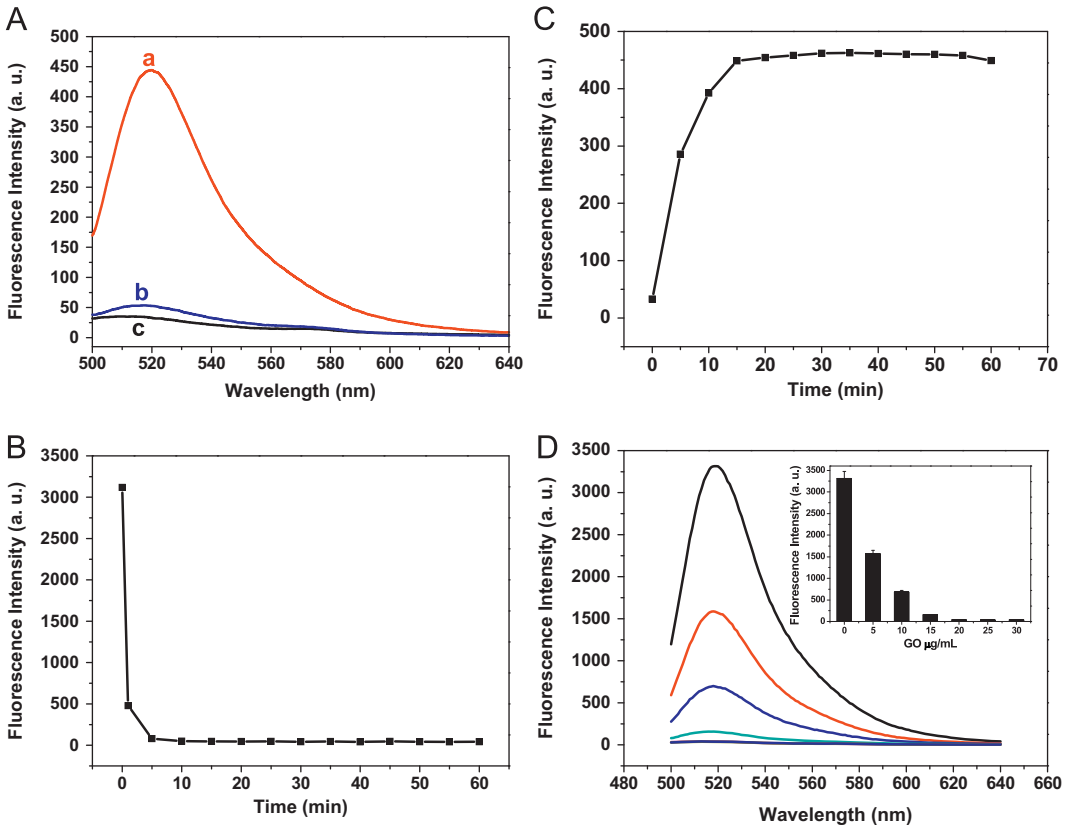


**Fig. 2.** Optimization of the assay conditions. (A) Comparison the fluorescence intensity caused by the adding order of MNase and GO. (a) FAM-labeled 20-mer ssDNA+$4\times10^{-4}$ units/mL MNase+GO; (b) FAM-labeled 20-mer ssDNA+GO+$4\times10^{-4}$ units/mL MNase; (c) FAM-labeled 20-mer ssDNA+GO. (B) Fluorescence quenching of FAM-labeled 20-mer ssDNA (40 nM) in Tris–HCl buffer by GO as a function of time. (C) Fluorescence intensity versus different reaction time of FAM-labeled 20-mer ssDNA (40 nM) with MNase ($4\times10^{-4}$ units/mL). (D) Fluorescence emission spectra of FAM-labeled 20-mer ssDNA (40 nM) upon the addition of different concentration of GO. Inset: fluorescence intensity versus concentration of GO. Excitation: 480 nm.

2010b). As a result, to achieve the sensing performance of MNase detection, MNase should be added before the addition of GO.

### 3.3. Effect of reaction time

After identifying the sensing platform system for this GO-based biosensor design, we are in the position to unravel the optimal reaction time between FAM-labeled 20-mer ssDNA and GO, and the optimal reaction time between FAM-labeled 20-mer ssDNA and MNase. Fig. 2B shows the fluorescence quenching of FAM-labeled 20-mer ssDNA in the presence of GO as a function of incubation time. FAM-labeled 20-mer ssDNA adsorption on the surface of GO is very fast at room temperature. The process of adsorption reaches equilibrium in 5 min. Fig. 2C shows fluorescence intensity versus different reaction time of FAM-labeled 20-mer ssDNA (40 nM) with MNase ($4\times10^{-4}$ units/mL). It indicates that the reaction of FAM-labeled 20-mer ssDNA with MNase becomes slower and is completed in about 15 min at 37 °C. So we introduced GO into the sensing solution after the system had reacted for 30 min at 37 °C.

### 3.4. Effect of the concentration of GO

To achieve the best sensing performance, the concentration of GO was optimized. As shown in Fig. 2D, fluorescence intensity of FAM-labeled 20-mer ssDNA decreases sharply as the concentration of GO increases from 0 to 30 μg/mL. When GO concentration is up to 20 μg/mL or larger, the fluorescence intensity of FAM is quenched down to 1% of original fluorescence signal. As a result, 20 μg/mL was taken as the optimized concentration for GO.

### 3.5. MNase detection in a Tris–HCl buffer with GO-based biosensor

In our experiment, this GO-based biosensor platform was used for MNase detection. Fig. 3A shows the fluorescence emission spectra of the GO-based biosensor in the presence of different concentrations of MNase. The fluorescence intensity of the biosensor dramaticly increases with the increasing concentration of MNase from $8\times10^{-5}$ to $1.6\times10^{-3}$ unit/mL. The calibration curve for MNase detection is shown in Fig. 3B, and the linear range is from $8\times10^{-5}$ to $1.6\times10^{-3}$ unit/mL with linear equation $y=4200x-1.05$, where y is the ratio of $F/F_0$ (where $F_0$ and $F$ are the fluorescence intensities of FAM at 520 nm in the absence and presence of MNase, respectively) and $x$ is the concentration of MNase (regression coefficient $R^2=0.9969$). The detection limit is estimated to be $2.7\times10^{-5}$ unit/mL ($3S_0/S$, in which $S_0$ is the standard deviation for the blank solution, $n=11$, and $S$ is the slope of the calibration curve), which is of two order of magnitude lower than those reported MNase biosensor based on QDs (Huang et al., 2008; Qiu et al., 2010). However, no obvious emission change could be observed from the FAM-labeled 20-mer ssDNA solution upon the increasing concentration of MNase from $8\times10^{-5}$ to $1.6\times10^{-3}$ unit/mL (shown in Fig. S3). Therefore, the above-mentioned experimental results demonstrate that this GO-based biosensor could be used as a sensitive approach for MNase detection. The reason that explains this excellent performance of this GO-based biosensor is that GO is an excellent energy acceptor in resonance energy transfer (Swathi and Sebastian, 2008, 2009),

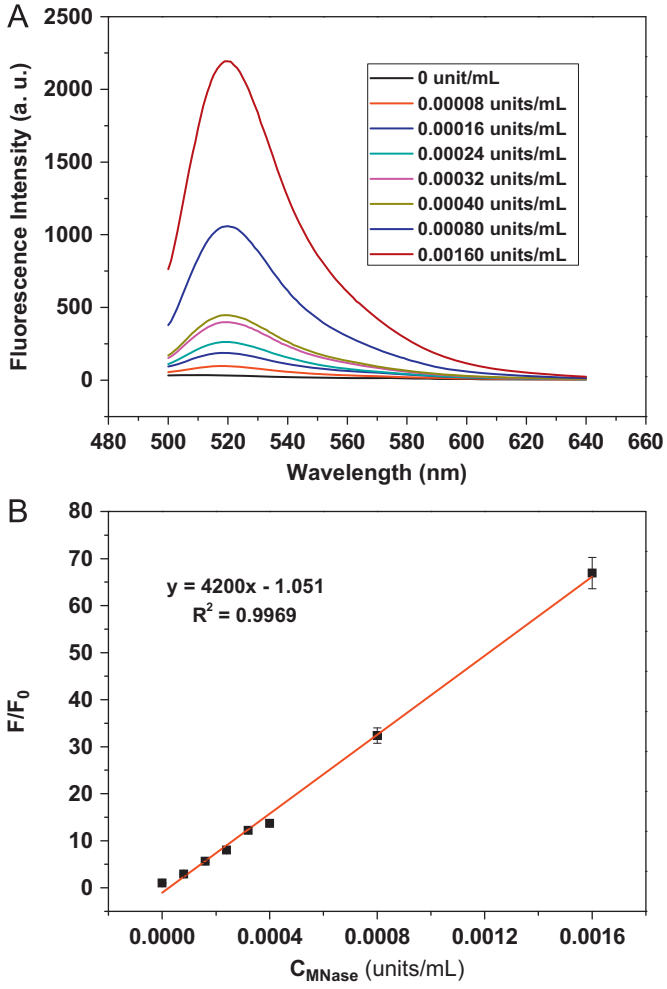


**Fig. 3.** Fluorescence emission spectra of GO-based biosensor in the presence of increasing amount of MNase (0, $8\times10^{-5}$, $1.6\times10^{-4}$, $2.4\times10^{-4}$, $3.2\times10^{-4}$, $4.0\times10^{-4}$, $8.0\times10^{-4}$ and $1.6\times10^{-3}$ unit/mL) and calibration curve for MNase detection. (A) Fluorescence emission spectra of GO-based biosensor upon the addition of MNase at different concentrations. (B) Calibration curve for MNase detection. Excitation: 480 nm.

which leads this GO-based biosensor to low background and results in high sensitivity.

### 3.6. Specificity of GO-based biosensor

In this study, under the optimized detection condition, other nucleases (S1 nuclease and exonuclease I) were selected to study the specificity of GO-based biosensor under the same conditions. The S1 nuclease also degrades single-stranded nucleic acids, releasing 5′-phosphoryl mono- or oligonucleotides. The excision of ssDNA by S1 nuclease has also occurred in AT-rich regions, which is similar to the cleavage site of MNase (Hofstetter et al., 1976). But, it has been reported that the S1 nuclease has its maximal activity at the acid pH (4.2) and requires $Zn^{2+}$ or $Co^{2+}$ for maximal activity (Vogt, 1973). Exonuclease I breaks apart single-stranded DNA in the direction 3′→5′, releasing deoxyribonucleoside 5′-monophosphates one after another. In a typical experiment, the FAM-labeled 20-mer ssDNA was incubated with $4.0\times10^{-3}$ unit/mL S1 nuclease, $4.0\times10^{-3}$ unit/mL exonuclease I, and $4.0\times10^{-4}$ unit/mL MNase 30 min at 37 °C, respectively. Then introduce GO into these sensing solution, respectively. As shown in Fig. 4, fluorescence of the GO-based biosensor changed less for S1 nuclease, and exonuclease I, while a significant fluorescence increase was observed

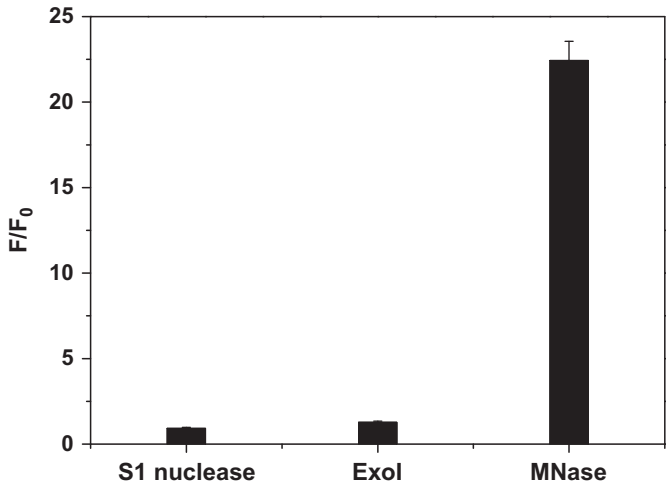


**Fig. 4.** Fluorescence intensity changes ($F/F_0$) of GO-based biosensor in the presence of S1 nuclease ($4.0\times10^{-3}$ unit/mL), exonuclease I ($4.0\times10^{-3}$ unit/mL), and MNase ($4.0\times10^{-4}$ unit/mL) respectively, where $F_0$ and $F$ are the fluorescence intensity of FAM at 520 nm in the absence and presence of S1 nuclease, exonuclease I, and MNase, respectively. Excitation: 480 nm.

for MNase. The relative fluorescence $F/F_0$ of the GO-based biosensor in the presence of MNase is 22.43, which is much higher than that of 0.93 for S1 nuclease, and 1.28 for exonuclease I, where $F_0$ and $F$ are the fluorescence intensity of the GO-based biosensor without and with S1 nuclease, exonuclease I, and MNase, respectively. These results validated the specificity of the GO-based biosensor for MNase testing.

### 3.7. MNase detection in culture medium

To demonstrate the potential application of the assay for MNase detection in real biological sample, the culture medium containing *S. aureus* (*S. aureus*) which could secrete MNase (Arnone et al., 1969) is selected as the real sample. It has been reported that existence of MNase can be the standard to identify *S. aureus* and the content of MNase can be used to evaluate the pathogenicity of *S. aureus* (Lachica, 1976; Lagacé-Wiens et al., 2007). As the culture medium may contain complex components such as inorganic salts, organic compounds, proteins or even large particles, if we wish to apply this GO-based biosensor to test the content of MNase secreted by *S. aureus*, we firstly need to investigate whether this GO-based biosensor can be used to detect MNase in culture medium. The interaction between GO and FAM-labeled 20-mer ssDNA in 0.4% culture medium was examined. Interestingly, the fluorescence of the FAM-labeled 20-mer ssDNA is rapidly quenched by GO as well, with the fluorescence quenching dependent on the ratio between FAM-labeled 20-mer ssDNA and GO. As shown in Fig. S4, fluorescence intensity of FAM-labeled 20-mer ssDNA decreases sharply as the concentration of GO increases from 0 to 60 μg/mL. When GO concentration is up to 40 μg/mL, fluorescence intensity of FAM is quenched down to 2% of the original fluorescence signal. As a result, 40 μg/mL was taken as the optimized concentration for GO. The fact that more GO is needed to quench equivalent FAM-labeled 20-mer ssDNA in 0.4% culture medium than that in clean Tris–HCl buffer may be attributed to the interaction between GO and some biomolecules in culture medium, which results in the reduction of interaction area and the enlargement of distance between the GO and FAM-labeled 20-mer ssDNA.

The detection process of MNase in 0.4% culture medium was the same as in the Tris–HCl buffer. Fig. 5 shows the changes of fluorescence intensity of FAM-labeled 20-mer ssDNA in different

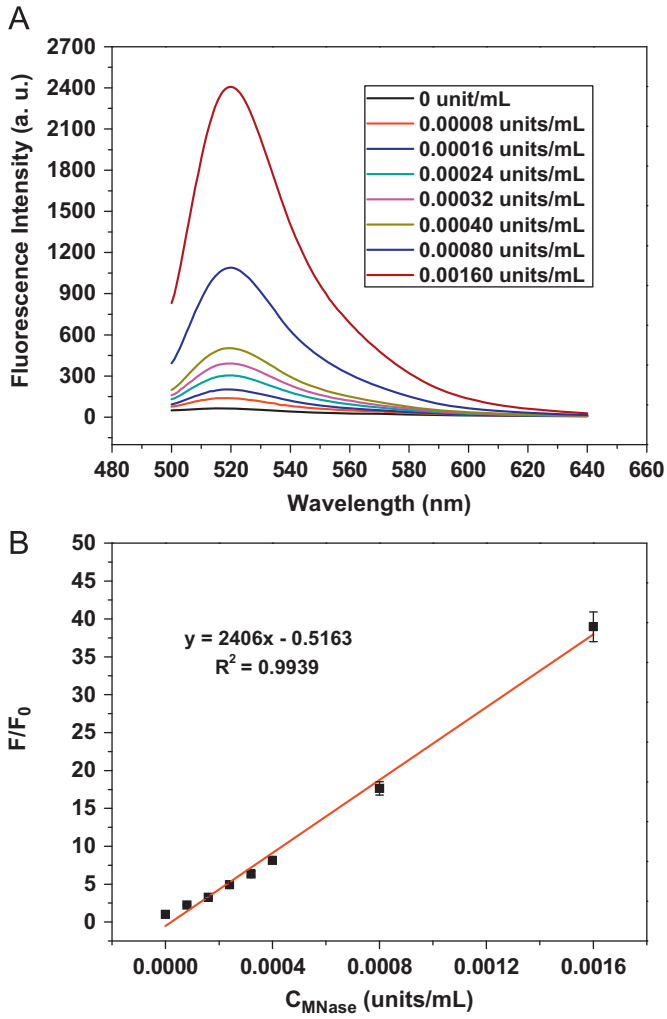


**Fig. 5.** Fluorescence emission spectra of GO-based biosensor in culture medium in the presence of increasing amount of MNase ($0.8\times10^{-5}$, $1.6\times10^{-4}$, $2.4\times10^{-4}$, $3.2\times10^{-4}$, $4.0\times10^{-4}$, $8.0\times10^{-4}$ and $1.6\times10^{-3}$ unit/mL) and calibration curve for MNase detection. (A) Fluorescence emission spectra of GO-based biosensor in culture medium upon the addition of MNase at different concentrations. (B) Calibration curve for MNase detection in culture medium. Excitation: 480 nm.

concentration of MNase in 0.4% culture medium. Fig. 5A shows the fluorescence emission spectra of GO-based biosensor in the presence of different concentrations of MNase. The fluorescence intensity of the biosensor increases with the increasing concentration of MNase. The calibration curve for MNase detection is shown in Fig. 5B, and the linear equation $y=2406x-0.5163$, where y is the ratio of $F/F_0$ (where $F_0$ and $F$ are the fluorescence intensities of FAM at 520 nm in the absence and presence of MNase, respectively) and $x$ is the concentration of MNase (regression coefficient $R^2=0.9939$). This clearly shows the GO-based biosensor can be used to detect MNase in culture medium sensitively.

### 3.8. Detection of MNase secreted by S. aureus

After optimizing and performing the sensing platform system in culture medium, we are in the position to detect MNase secreted by *S. aureus*. Since the synthesis and secretion of MNase can be completed within 8 h in culture medium containing the *S. aureus* at 37 °C (Otero et al., 1988, 1990), the fluorescence spectra of the GO-based biosensor in four culture mediums (one culture medium contains *S. aureus* just inoculated; the others contain *S. aureus* which has been incubated for 2 h, 4 h, 6 h and

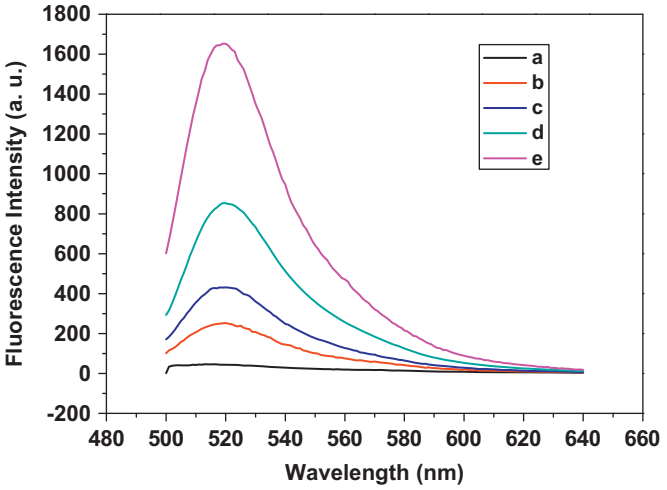


**Fig. 6.** Fluorescence emission spectra of GO-based biosensor (a) the *S. aureus* culture medium without incubating, (b) the *S. aureus* culture medium incubated for 2 h, (c) the *S. aureus* culture medium incubated for 4 h, (d) the *S. aureus* culture medium incubated for 6 h and (e) the *S. aureus* culture medium incubated for 8 h. Excitation: 480 nm.

8 h at 37 °C, respectively) were recorded. As shown in Fig. 6, the fluorescence intensity of the GO-based biosensor was gradually increased with the increase of the incubated time (with the increase of MNase). The concentration of MNase in the culture medium contains *S. aureus* incubated for 2 h is $0.46\pm0.05$ unit/mL ($n=3$), incubated for 4 h is $0.91\pm0.04$ unit/mL ($n=3$), incubated for 6 h is $1.55\pm0.02$ unit/mL ($n=3$) and incubated for 8 h is $3.05\pm0.04$ unit/mL ($n=3$) (Table S1). The recovery was tested by the standard addition method (Table S2). The recoveries for the determination of MNase are in the range from 97.9% to 103%, indicating that the proposed fluorescent GO-based biosensor for MNase can be used in real sample analysis.

Good precision and reproducibility are also important criteria for further application of the method. Here, samples contains *S. aureus* incubated for 2 h, 4 h, 6 h, and 8 h were detected five times, respectively, and the within-day assay variability (Table S3) was calculated by the means of the coefficient of variation (CV=SD/mean) of the four results. The within-day assay variability of 0.49% proved the good precision and the good reproducibility of this method. To further confirm the reproducibility, the between-day assay variability was tested as in the same way, with the variability of 2.46%. This clearly shows the GO-based biosensor can be used to detect MNase in practical samples sensitively, reproducibility and might be a promising probe for MNase secreted by *S. aureus* assay.

## 4. Conclusion

In summary, a simple and ultra-high sensitive strategy for micrococcal nuclease (MNase) detection using GO-based biosensor is developed in this work, simply utilizing the difference in affinity of graphene oxide (GO) for single-stranded DNA containing different numbers of bases in length. The dye-labeled ssDNA is adsorbed on the surface of GO via π–π stacking interactions, resulting in the quenching of fluorescence due to energy transfer between dye-labeled ssDNA and GO. Upon the addition of MNase, the dye-labeled ssDNA was cleaved into small fragments. The introduction of GO into the sensing solution results in weak quenching of the fluorescence of the dyes due to the weak affinity of the short dye-linked oligonuleotide fragment to GO, and the fluorescence intensity gradually increases with increasing

concentration of MNase. With such a straightforward design, quantitative determination of MNase can be performed with quite good analytical performances. This method could be extended to the assay of the MNase secreted by *Staphylococcus aureus* (*S. aureus*). The recoveries, precision and reproducibility of *S. aureus* samples analysis are satisfactory. In addition, the new strategy is featured with high simplicity. Therefore, we can reasonably expect that the GO-based biosensor model can be readily developed for other nucleases whose substrates are ssDNA molecules such as S1 nuclease just by changing the reaction buffer.

## Acknowledgments

This work was supported by the National Basic Research Program of China (973 Program, Nos. 2011CB933600 and 2006CB933100), the Science Fund for Creative Research Groups of NSFC (Nos. 20621502 and 20921062), the National Natural Science Foundation of China (21275110; 20833006; 20875071; 21005056), and the Fundamental Research Funds for the Central Universities (20100141110015).

## Appendix A. Supporting information

Supplementary data associated with this article can be found in the online version at http://dx.doi.org/10.1016/j.bios.2012.10.045.

## References

Allan, J., Fraser, R.M., Owen-Hughes, T., Keszenman-Pereyra, D., 2012. Journal of Molecular Biology 417, 152–164.
Arber, W., 1978. Angewandte Chemie International Edition 17, 73–79.
Arnone, A., Bier, C.J., Cotton, F.A., Hazen Jr, E.E., Richardson, D.C., Richardson, J.S., 1969. Proceedings of the National Academy of Sciences of the United States of America 64, 420–427.
Bouriotis, V., Zafeiropoulos, A., Clonis, Y.D., 1987. Analytical Biochemistry 160, 127–134.
Cao, R., Li, B.X., Zhang, Y.F., Zhang, Z.N., 2011. Chemical Communications 47, 12301–12303.
Chang, H.X., Tang, L.H., Wang, Y., Jiang, J.H., Li, J.H., 2010. Analytical Chemistry 82, 2341–2346.
Feng, X.L., Duan, X.R., Liu, L.B., Feng, F.D., Wang, S., Li, Y.L., Zhu, D.B., 2009. Angewandte Chemie International Edition 121, 5420–5425.
Fox, K.R., Waring, M.J., 1987. Biochimica et Biophysica Acta-Gene Structure and Expression 909, 145–155.
Geim, A.K., Novoselov, K.S., 2007. Nature Materials 6, 183–191.
Hiramatsu, K., Miura, H., Kamei, S., Iwasaki, K., Kawakita, M., 1998. Journal of Biochemistry 124, 231–236.
Hofstetter, H., Schamböck, A., Van Den Berg, J., Weissmann, C., 1976. Biochimica et Biophysica Acta—Nucleic Acids and Protein Synthesis 454, 587–591.
Huang, S., Xiao, Q., He, Z.K., Liu, Y., Tinnefeld, P., Su, X.R., Peng, X.N., 2008. Chemical Communications, 5990–5992.
Lachica, R.V.F., 1976. Applied and Environment Microbiology 32, 633–634.
Lagacé-Wiens, P.R.S., Alfa, M.J., Manickam, K., Karlowsky, J.A., 2007. Journal of Clinical Microbiology 45, 3478–3479.
Lee, J., Min, D.H., 2012. Analyst 137, 2024–2026.
Liu, M., Zhao, H.M., Chen, S., Yu, H.T., Quan, X., 2012. Acs Nano 6, 3142–3151.
Lu, C.H., Li, J.A., Lin, M.H., Wang, Y.W., Yang, H.H., Chen, X., Chen, G.N., 2010a. Angewandte Chemie International Edition 122, 8454–8457.
Lu, C.H., Li, J., Qi, X.J., Song, X.R., Yang, H.H., Chen, X., Chen, G.N., 2011. Journal of Materials Chemistry 21, 10915–10919.
Lu, C.H., Yang, H.H., Zhu, C.L., Chen, X., Chen, G.N., 2009. Angewandte Chemie International Edition 48, 4785–4787.
Lu, C.H., Zhu, C.L., Li, J., Liu, J.J., Chen, X., Yang, H.H., 2010b. Chemical Communications 46, 3116–3118.
Nishino, T., Morikawa, K., 2002. Oncogene 21, 9022–9032.
Norberg, P., Bergstrom, T., Liljeqvist, J.A.J., 2006. Clinical Microbiology 44, 4511–4514.
Novoselov, K.S., Geim, A.K., Morozov, S.V., Jiang, D., Zhang, Y., Dubonos, S.V., Grigorieva, I.V., Firsov, A.A., 2004. Science 306, 666–669.
Otero, A., García, M.C., Moreno, B., 1988. Journal of Food Microbiology 6, 107–114.
Otero, A., García, M.L., García, M.C., Moreno, B., Bergdoll, M.S., 1990. Applied and Environment Microbiology 56, 555–559.
Pingoud, A., Jeltsch, A., 2001. Nucleic Acids Research 29, 3705–3727.
Pu, F., Hu, D., Ren, J.S., Wang, S., Qu, X.G., 2010. Langmuir 26, 4540–4545.
Qiu, T., Zhao, D., Zhou, G.H., Liang, Y.A., He, Z.K., Liu, Z.H., Peng, X.N., Zhou, L., 2010. Analyst 135, 2394–2399.
Rosenthal, A.L., Lacks, S.A., 1977. Analytical Biochemistry 80, 76–90.
Smith, J., Anslyn, E.V., 1994. Analytical Biochemistry 220, 53–57.
Song, G.T., Chen, C., Ren, J.S., Qu, X.G., 2009. ACS Nano 3, 1183–1189.
Stoerker, J., Mayo, J.D., Tetzlaff, C.N., Sarracino, D.A., Schwope, I., Richert, C., 2000. Nature Biotechnology 18, 1213–1216.
Swathi, R.S., Sebastian, K.L., 2008. Journal of Chemical Physics 129, 054703.
Swathi, R.S., Sebastian, K.L., 2009. Journal of Chemical Physics 130, 086101.
Tang, Y.L., Feng, F.D., He, F., Wang, S., Li, Y.L., Zhu, D.B., 2006. Journal of the American Chemical Society 128, 14972–14976.
Vogt, V.M., 1973. European Journal of Biochemistry 33, 192–200.
Wright, D.A., Townsend, J.A., Winfrey, R.J., Irwin, P.A., Rajagopal, J., Lonosky, P.M., Hall, B.D., Jondle, M.D., Voytas, D.F., 2005. Plant Journal 44, 693–705.
Xu, X.Y., Han, M.S., Mirkin, C.A., 2007. Angewandte Chemie International Edition 46, 3468–3470.
Zeevi, V., Tovkach, A., Tzfira, T., 2008. Proceedings of the National academy of Sciences of the United States of America 105, 12785–12790.
Zhang, Y., Wang, Y.Y., Liu, B., 2009. Analytical Chemistry 81, 3731–3737.
Zhao, X.H., KOng, R.M., Zhang, X.B., Meng, H.M., Liu, W.N., Tan, W.H., Shen, G.L., Yu, R.Q., 2011. Analytical Chemistry 83, 5062–5066.